

1 **Climate change implications in the suitable habitat of Olive ridley turtle *Lepidochelys olivacea***
2 **in the Eastern Tropical Pacific**

3 Elka García-Rada^{a,b,c}, Aura Buenfil-Ávila^a, Christine Figgenger^d, Héctor M. Guzmán^{b,e}, Pamela
4 T. Plotkin^f, Gabriel Reygondeau^g, Carlos Robalino-Mejía^{a,b,c}, Derek P. Tittensor^h, Héctor
5 Villalobos^{a*} & César Peñaherrera-Palma^b

6

7 ^aInstituto Politécnico Nacional - Centro Interdisciplinario de Ciencias Marinas, Av. IPN s/n Col.
8 Playa Palo de Sta. Rita, La Paz, B.C.S., México

9 ^bMigraMar, 2099 Westshore Rd, Bodega Bay, CA 94923

10 ^cPelagios Kakunjá, a.C., La Paz, B.C.S., Mexico

11 ^dCosta Rican Alliance for Sea Turtle Conservation & Science

12 ^e Smithsonian Tropical Research Institute, Naos Marine Laboratory, Panama

13 ^fTexas Sea Grant

14 ^gDepartment of Marine Biology and Ecology, Rosenstiel School of Marine, Atmospheric, and
15 Earth Science, University of Miami, 4600 Rickenbacker Causeway, Miami, FL 33149, USA

16 ^hDalhousie University, Halifax, Canada

17 *Corresponding author: hvillalo@ipn.mx

18

19 Elka García Rada <https://orcid.org/0000-0003-2971-5504>

20 Héctor Villalobos <https://orcid.org/0000-0002-6424-4050>

21 Héctor Guzmán <https://orcid.org/0000-0001-9928-8523>

22 Christine Figgenger <https://orcid.org/0000-0002-8321-229X>

23 Pamela Plotkin <https://orcid.org/0000-0003-3973-8988>

24 Gabriel Reygondeau <https://orcid.org/0000-0001-9074-625X>

25 Aura Buenfil <https://orcid.org/0000-0002-6586-6476>

26 Carlos Robalino Mejía <https://orcid.org/0000-0001-5647-6356>

27 Derek P. Tittensor <https://orcid.org/0000-0002-9550-3123>

28 César Peñaherrera Palma <https://orcid.org/0000-0002-6621-201X>

29

30 **Abstract**

31 We model the habitat suitability of *Lepidochelys olivacea* in the Eastern Tropical Pacific using
32 remote sensing data from 59 individuals tagged in Panama and Costa Rica between 2009 and
33 2018. The response was modeled with MaxEnt, using a presence-only approach and
34 environmental variables including sea surface temperature, ocean mixed layer thickness,
35 chlorophyll-a concentration, and current velocity. The model categorized months into cold
36 (El Niño) and warm (La Niña) conditions, providing insight into climate change effects. Results
37 reveal that chlorophyll-a concentration and sea surface temperature best predicted the

38 presence of *L. olivacea*. The intertropical convergence zone exhibited high habitat suitability,
39 especially in the Central Pacific. During El Niño, suitable habitat declined, primarily along
40 coastlines, while, during La Niña, it expanded, favoring oceanic waters and temperate
41 temperatures in upwelling zones. These findings suggest climate change could significantly
42 impact *L. olivacea* distribution, potentially shifting nesting and foraging areas.

43 **Keywords:** MaxEnt, ENSO, habitat, marine ecology, Maximum entropy, modeling.

44 1. Introduction

45 The olive ridley turtle *Lepidochelys olivacea* is considered the most abundant of all marine
46 turtle species ([Abreu-Grobois and Plotkin, 2008](#)). It inhabits tropical and subtropical waters
47 in the Pacific, Atlantic, and Indian Oceans ([Whiting et al., 2007](#)). Its habitat use has been
48 observed to be either neritic or oceanic, depending on the population and also likely,
49 depending on prey availability variations among regions ([Plotkin, 2010](#); [Polovina et al., 2003](#)).
50 For example, studies in Australia have revealed that female olive ridley turtles do not
51 undertake extensive migratory movements but remains in neritic waters close to their
52 nesting sites ([McMahon et al., 2007](#); [Whiting et al., 2007](#)). Similarly, along the coast of French
53 Guiana, this species remains above the continental shelf in areas with high abundance of
54 food as a result of the formation of eddies ([Chambault et al., 2016](#)). Conversely, juvenile
55 olive ridley turtles observed near Hawaii have been shown to belong to distinct western and
56 eastern Pacific populations and to be associated with warmer oceanic waters in the center
57 of the subtropical gyre ([Polovina et al., 2003](#)). In the Eastern Tropical Pacific (ETP), females
58 exhibit long yet nomadic oceanic migratory behaviors characterized by non-directional
59 movements ([Plotkin, 2010](#); [Swimmer et al., 2009](#)). Recent studies suggest that in this region
60 olive ridley turtles spend 30% of their time migrating and 70% foraging in oceanic areas
61 searching for food ([Guzman et al., 2019](#)), with core utilization areas off the coast from
62 Guatemala to Panama ([Figgner et al., 2022](#)).

63 In 2008, the International Union for Conservation of Nature (IUCN) classified the olive ridley
64 turtle as vulnerable based on an estimated global population decline of approximately 30%
65 ([Abreu-Grobois and Plotkin, 2008](#)). Although a new evaluation is pending to assess its current
66 conservation status, the olive ridley remains exposed to negative impacts derived from
67 multiple human stressors including climate change, bycatch environmental pollution, and
68 habitat loss ([Caceres-Farias et al., 2022](#)). Among all these threats, climate change represents
69 a growing challenge to conservation efforts for this species ([Root et al., 2003](#)), as it is for
70 marine ecosystems and biodiversity more generally ([IPBES, 2019](#)). In part, this comes from a
71 knowledge gap regarding the response strategies of *Lepidochelys olivacea* to specific regional
72 changes in environmental factors. Climate change is predicted to affect marine turtles by
73 influencing their metabolic rates ([Patrício et al., 2019](#)), sex ratios ([Maurer et al., 2021](#)),
74 migration patterns ([Quiñones et al., 2010](#)), and phenological cycles ([Ariano-Sánchez et al.,
75 2020](#)). Studies have shown that prolonged warm periods by rising global temperatures can
76 decrease reproductive frequency and hatching success, as observed in *Dermochelys coriacea*
77 (leatherback sea turtle) in the ETP ([Saba et al., 2008](#); [Santidrián et al., 2012](#)), or alter the
78 distribution of nesting sites as seen in *Caretta caretta* (loggerhead) in the Mediterranean Sea

79 ([Mancino et al., 2022](#)). Additionally, projected sea-level rise is expected to impact existing
80 nesting sites, potentially leading to the loss of critical nesting habitats and necessitating shifts
81 in nesting locations ([Simantiris, 2024](#)). However, no relationship between these events and
82 the abundance of females has yet been reported during the nesting season of *Lepidochelys*
83 *olivacea* ([Santidrián-Tomillo et al., 2020](#)). Climate change is projected to contribute to the
84 population growth of marine turtle species through population feminization ([Patrício et al.,](#)
85 [2019](#)). Uncertainty around the scope of these individual- and population-level impacts is
86 contingent upon and interacts with how suitable habitat for this species will be altered or
87 shift, likely towards higher latitudes. This may affect the suitability of existing nesting sites
88 and, furthermore, affect the distance this species has to travel from nesting to feeding
89 grounds and vice versa ([Caceres-Farias et al., 2022](#)). The resulting conservation risk for this
90 species increases when other anthropogenic activities (such as fisheries) overlap with
91 present or future high-use areas ([Montero et al., 2016](#)), emphasizing the critical need for a
92 nuanced and multi-faceted understanding of this species' responses to environmental
93 conditions.

94 Unequivocal evidence has shown global oceans are warming under human influence ([IPCC,](#)
95 [2021](#)). This warming has widespread implications, including rising sea levels, changes in
96 ocean productivity, and more extreme weather events. However, certain areas in the world
97 are experiencing the cooling of their waters ([Belkin, 2009](#)). The ETP exemplifies these
98 contrasting trends, with most of its coastal and oceanic waters showing significant warming
99 while localized upwelling areas have shown significant seasonal or decadal cooling ([Zevallos-](#)
100 [Rosado et al., 2023](#)). The observed divergent trends are partly due to the recurrence of El
101 Niño Southern Oscillation (ENSO) events, whose warm and cold phases have increased in
102 both frequency and intensity. This anticipated increase in ENSO frequency suggests that El
103 Niño and La Niña phases may occur more often and with greater variability in timing,
104 particularly if global mean temperatures rise 1.5°C above pre-industrial levels ([Cai, 2014;](#)
105 [Wang et al., 2017](#)). Furthermore, these increasingly extreme processes can result in
106 significant changes to sea surface temperature and impact ocean productivity ([Cai, 2014;](#)
107 [McPhaden et al., 2009;](#) [Zevallos-Rosado et al., 2023](#)). Because strong ENSO events can
108 change environmental variables, they can limit and change the distribution of migratory
109 species by changing their preferred habitat conditions and distribution of prey items ([Wang](#)
110 [and Fiedler, 2006](#)), as predicted to occur under climate change ([McPhaden et al., 2020](#)).
111 Thus, understanding ENSO effects on suitable habitats could shed light on future responses
112 of species such as *Lepidochelys olivacea* to a changing environment and the potential impacts
113 of climate change on marine life.

114 As an approach to exploring the impacts of climate change on species habitat and
115 distributions, species distribution models (SDM) are gaining popularity ([Pearson and Dawson,](#)
116 [2003](#)), allowing evaluation of changes in habitat suitability through a habitat index (HSI) using
117 only presence data ([Jiménez-Valverde et al., 2011](#)). The use of SDM has provided important
118 insights into the spatial ecology of many species, including sea turtles, across diverse global
119 regions. These models have facilitated the identification of critical habits for species such as
120 *Caretta caretta* in the Mediterranean ([Guo, 2014](#)), *Lepidochelys olivacea* on the Atlantic coast

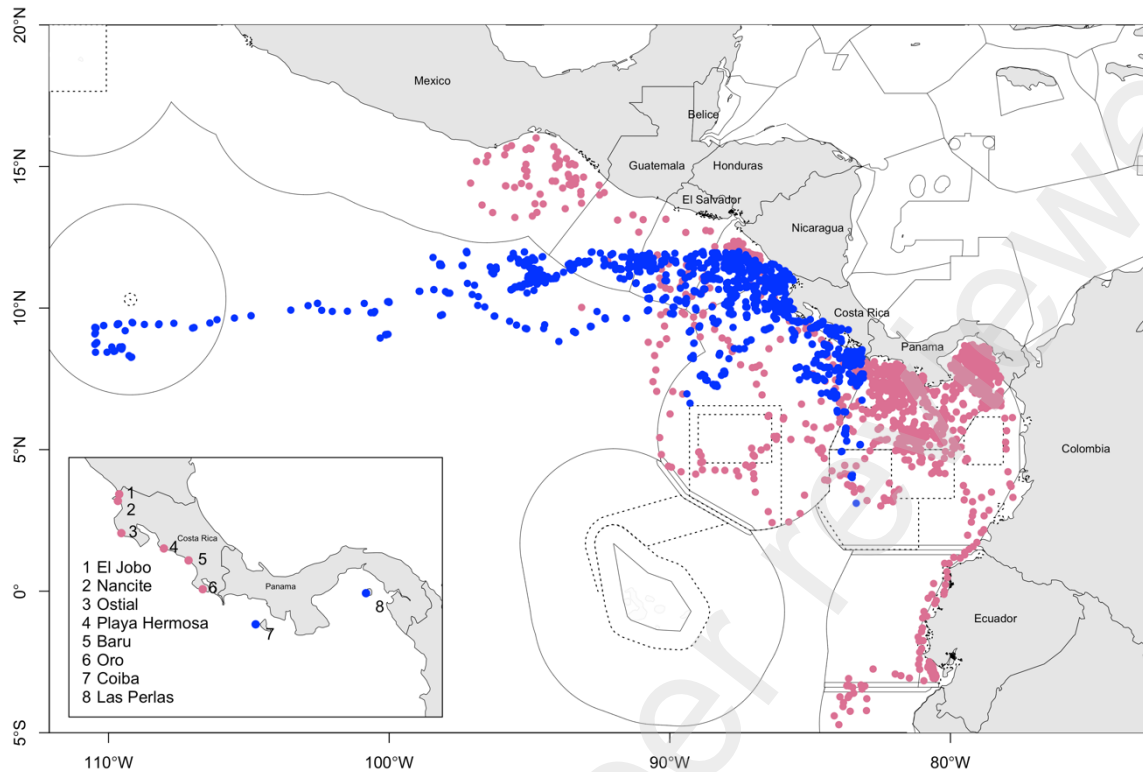
121 of Central Africa ([Pikesley et al., 2013](#)), *Dermochelys coriacea* in the ETP ([Costanza et al.,](#)
122 [2021](#); [Dávalos, 2021](#)), *Chelonia mydas* in the southwestern Atlantic Ocean ([Carman et al.,](#)
123 [2016](#)), and *Lepidochelys kempii* in the Gulf of Mexico ([Fujisaki et al., 2020](#)). These studies
124 reveal differing habitat preferences among species, highlighting the need for species-specific
125 models that incorporate data from various life stages and activities such as migration,
126 reproduction, and foraging to enhance model accuracy. By recognizing these individual
127 habitat preferences, we can develop more accurate models that reflect the true diversity of
128 migratory behavior among marine turtles.

129 At present, a lack of understanding of the effect of climate variability (e.g., ENSO events),
130 coupled with its nomadic migratory behavior, makes conservation efforts on *Lepidochelys*
131 *olivacea* extremely complex in the ETP. Our study aims to describe the habitat suitability of
132 the olive ridley turtle *Lepidochelys olivacea* in the ETP, determine the oceanographic
133 conditions associated with its distribution, and assess the impact of past ENSO events on its
134 distribution patterns along the Pacific coast of Central and South America, thus shedding
135 light on potential impacts of climate change. Harnessing SDM derived from satellite-
136 telemetry and local individual tracking offers an opportunity to close the understanding gap
137 on how *Lepidochelys olivacea* responds to specific regional changes in environmental
138 variables, allowing for a comprehensive spatiotemporal exploration of how climatic
139 variability may shape the distribution of this turtle. It also provides insight into how increasing
140 global temperatures could impact this species' distribution.

141 2. Materials and methods

142 2.1. Study Area

143 The study area is in the Eastern Tropical Pacific (ETP) between latitudes 8° S - 20° N and
144 longitudes 75° W – 110° W and includes the coasts of Mexico, Guatemala, El Salvador,
145 Nicaragua, Costa Rica, and Ecuador (Fig. 1). This region is influenced by equatorial currents
146 from the north and south that flow westward and are derived from the temperate currents
147 of California and Humboldt, respectively ([Pennington et al., 2006](#)). Along the coast from
148 southeastern Mexico to Panama, temperatures in the ETP exceed 25 °C, while relatively
149 cooler waters (< 25 °C) are found to the west in the adjacent waters of the Baja California
150 Peninsula north and south of the equatorial line in Ecuador and Peru ([Zevallos-Rosado et al.,](#)
151 [2023](#)). The oceanographic dynamics of this region are influenced by winds that generate
152 nearshore eddies that affect sea surface temperature and circulation ([Pennington et al.,](#)
153 [2006](#)). Major mesoscale features include cyclonic and anticyclonic eddies in the Gulf of
154 Panama, Costa Rica dome, and the Gulf of Tehuantepec, which originate offshore of Panama,
155 Costa Rica, and southern Mexico, respectively. These features are the result of strong, highly
156 seasonal wind gusts that deliver nutrients to marine areas located up to 1000 km offshore
157 ([Lavín et al., 2006](#); [Rodríguez-Zárate et al., 2018](#)). These key features are thought to generate
158 biological hotspots that make this region one of the most biodiverse in the world ([Rodríguez-](#)
159 [Zárate et al., 2018](#); [Seminoff et al., 2012](#)).



160

161 **Fig. 1.** Map of the study area. Main panel, olive ridley post-nesting movements based on
 162 satellite-tagged individuals in Panama (2009-2011, blue dots) by [Guzman et al. \(2019\)](#) and in
 163 Costa Rica (2016-2018, pink dot) by [Figgenger et al. \(2022\)](#). Inset, tagging locations along the
 164 coast of coast Costa Rican and Panamanian coasts; Solid lines, exclusive economic zones;
 165 Dashed lines, marine protected areas.

166 2.2. Data collection

167 2.2.1. Telemetry data

168 In this study, satellite telemetry data published by [Guzman et al. \(2019\)](#) and [Figgenger \(2022\)](#)
 169 were used, comprising a total of 59 adult individuals (51 females and eight males) during the
 170 nesting season (June – December). [Guzman et al. \(2019\)](#) tagged 34 adult olive ridley turtles
 171 (26 females and eight males) between 2009 and 2021 on Panamanian beaches and
 172 surrounding waters in the Las Perlas Archipelago, Gulf of Panama. and the Coiba National
 173 Park, Gulf of Chiriquí. [Figgenger et al. \(2022\)](#) tagged 35 female turtles between 2016 and 2018
 174 in six Costa Rican beaches: El Jobo, Nancite, Ostional, Playa Hermosa, Barú, and Río Oro (see
 175 Fig. 1).

176 All individuals were equipped with a satellite transmitter that broadcasted the location
 177 (latitude and longitude) of the turtle after its release. Different types of transmitters were
 178 used: SPOTT5 AM-S244A in 2009 – 2011 (n=34, Wildlife Computers Inc.); SeaTagTT in 2016
 179 (n=7, Deserts Star LLC); SeaTrkr-4370-4 in 2017 (n=2, Telonics Inc.). Transmitters were
 180 approximately 6 cm long and had an approximate weight of 270 g, which is < 1% of an adult

181 turtle's body weight. Female turtles were immobilized on nesting beaches after egg-laying.
182 Males were captured on the reefs surrounding the nesting beaches. Devices were placed on
183 the highest point of each turtle's shell, ensuring the antenna pointed towards the animal's
184 back. The transmitter was attached with epoxy glue and then painted with anti-fouling paint.
185 From 2009 to 2011, transmitters were programmed to transmit data every hour. The 2016
186 transmitters were solar-powered and remained continuously active. The 2017 and 2018
187 devices were set to have a transmission cycle of 6 hours on and 50 hours off, and 6 hours on
188 and 58 hours off, respectively, and transmitted between 11:00-17:00 and 19:00-01:00
189 Coordinated Universal Time (UTC). Turtle's movements were monitored by the Argos and
190 IRIDIUM systems and subsequently imported into the SEATURTLE.ORG satellite tracking and
191 analysis tool ([Coyne and Godley, 2005](#)).

192 All relocations with a precision classification of "Z" (unknown location) were removed from
193 the dataset to ensure data quality. In addition, any value that indicated a speed of > 5 km/h
194 was discarded according to the procedures established by [Rees et al. \(2012\)](#). The remaining
195 data have an approximate maximum spatial location error of about 1 km. To avoid spatial
196 and temporal autocorrelation of satellite telemetry data, we followed [Edrén et al. \(2010\)](#) to
197 1) exclude all satellite positions from the first 48 hours after tagging the individuals, and 2)
198 use a random selection of a fixed number of relocations from each tagged individual. All
199 analyses were performed using the R programming language ([R Core Team, 2023](#)).

200 **2.2.2. Environmental data**

201 Environmental variables were obtained from the Copernicus Marine Environment
202 Monitoring Service. Variables included sea surface temperature (°C), salinity (unitless),
203 chlorophyll-a concentration (mg m^{-3}), ocean mixed layer thickness (m), sea surface height
204 above geoid (m), and zonal (UO) and meridional (VO) components of current velocity (m s^{-1}).
205 These variables were selected because they collectively provide a comprehensive
206 understanding of the marine environment that influences the habitat behavior of
207 *Lepidochelys olivacea*. Sea surface temperature and salinity are crucial for assessing
208 physiological conditions and habitat suitability ([Esteban et al., 2020](#); [Olson et al., 2022](#)).
209 Chlorophyll-a concentration indicates the availability of primary production, which is vital for
210 understanding prey distribution ([Richardson et al., 2003](#)). The mixed layer thickness helps in
211 understanding nutrient availability and the vertical distribution of temperature ([Xue et al.,](#)
212 [2021](#)). The sea surface height is used as a proxy for frontal systems, which are important for
213 understanding the distribution of nutrients and prey ([Graham, 2014](#)). Finally, the current
214 velocity components facilitated the analysis of migration pathways and oceanic transport
215 dynamics that affect the species' distribution and behavior ([Luschi et al., 2003](#)). These
216 variables were downloaded as monthly averages from 1997 to 2021 for the study area. Data
217 for all variables except chlorophyll-a were obtained from Copernicus at a spatial resolution
218 of 9.2 km ([Dréville et al., 2022](#)). Chlorophyll-a was downloaded from the Global Ocean
219 Chlorophyll database with a spatial resolution of 4.6 km ([Colella et al., 2022](#)). Chlorophyll-a
220 data were spatially averaged to pixels of 9.2 km to ensure consistency among environmental
221 layers. Current velocity (CUR) was calculated as the result vector from the components UO

222 and VO following the formula $CUR = \sqrt{UO^2 + VO^2}$ by making use Pythagorean theorem. In
223 addition, to include only one variable associated with the current, the cosine sign of the
224 direction (in degrees) associated with the velocity of the currents was used. In this way,
225 velocities with directions between 0°-90° and 270°-360°, i.e. predominantly northwards, are
226 positive, while directions between 90°-270° (south) are negative.

227 To analyze long-term trends and ensure robustness in our results, we built climatology layers
228 of the environmental variables by averaging those for periods 2009-2011 and 2016-2018,
229 which represented the years with available telemetry data. The processing of all
230 environmental databases and the extraction of the values matching the turtle's locations was
231 done using the **satin** R package ([Villalobos and González-Rodríguez, 2020](#)). The inclusion of
232 highly correlated environmental variables can affect the perception and interpretation of
233 models ([Huang et al., 2011](#)). To avoid this, correlations between available environmental
234 variables were examined with the **virtualespecies** package ([Leroy et al., 2015](#)), which
235 computes them directly from the spatial matrices. The variables with a Pearson correlation
236 coefficient of > 0.5 were eliminated from further analyses. Since a high correlation was found
237 between sea surface temperature and salinity (p= -0.58; see Appendix 1), the latter was
238 excluded from the following SDM analysis. The correlation (in absolute value) for all the other
239 variables was between 0.04 and 0.5.

240 Finally, to meet the requirements of the specific SDM algorithm used here, namely MaxEnt,
241 all environmental variables were exported from R in ASCII format. These text files contain a
242 header with information about the number of columns and rows of the environmental data
243 matrix, the coordinates of the upper left corner of the matrix, and the cell size (spatial
244 resolution), followed by the values of the individual cells that make up the raster layer.

245 **2.3. *Lepidochelys olivacea* ecological niche model**

246 The maximum entropy algorithm (MaxEnt, v3.3.3; ([Phillips et al., 2006](#)) was used to develop
247 the SDM through the **kuenm** package ([Cobos et al., 2019](#)). This package can generate many
248 candidate models with different calibration configurations (class features, regularization
249 multipliers, and sets of environmental variables) to obtain a species-specific
250 parameterization. Before the calibration process, a bipartition of the presence datasets was
251 performed using the *get.checkerboard1* function from the **ENMeval** package to enable a
252 cross-validation approach ([Muscarella et al., 2014](#)). This function allowed us to partition the
253 presence datasets according to the grid pattern of a checkerboard throughout the study
254 area. Following this, 50% of the data was randomly selected for calibration and the remaining
255 50% for model validation. Finally, while MaxEnt does not require absence data, it does need
256 pseudo-absence background points. For this reason, 1839 background points (same
257 presences) were selected at random.

258 **2.3.1. Modeling parameters**

259 The calibration process to create candidate models was performed by parameter fitting with
260 the *kuenm_cal* function based on three class features: linear model (L), linear-quadratic

261 model (LQ), and linear-quadratic-hinge model (LQH). Class features are defined as
262 transformations applied to the different covariates used in the models to allow the modeling
263 of complex relationships ([Elith et al., 2011](#)). In addition, five values for the regularization
264 multiplier (1, 2, 4, 6, and 8) were chosen to define different levels of complexity and avoid
265 overfitting the data, as recommended by [Morales et al. \(2017\)](#). For each parameter
266 configuration, two models were created, one based on the entire dataset and the other
267 based solely on the training data. The former is used to calculate model complexity, and the
268 latter is used to calculate model performance and omission rates ([Cobos et al., 2019](#)). In
269 addition, the jackknife procedure was used to determine the relative contribution of each
270 environmental variable ([Phillips et al., 2006](#)).

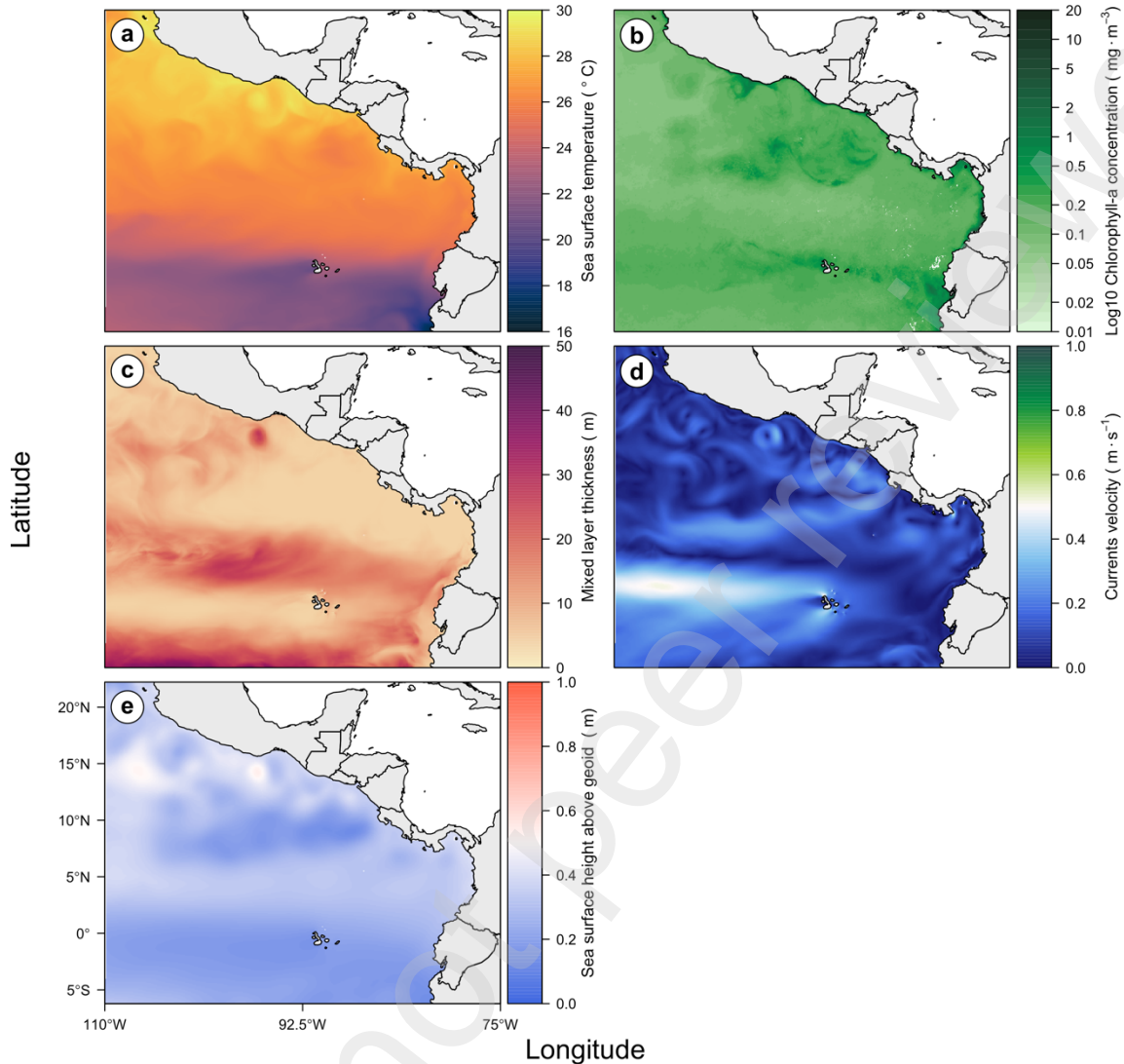
271 Validation and selection of the final model was performed using the *kuenm_ceval* function.
272 This function selects models by cross-validation based on three main criteria: (1) the area
273 under the partial receiver operating characteristic curve (ROCp), (2) the omission rate (< 5%),
274 and (3) the Akaike Information Criterion corrected for small sample sizes (AICc). We specified
275 a cumulative output for the final model representation before repeating the bootstrapping
276 and MaxEnt procedure 100 times. The variation in model performance metrics, such as AUC
277 and TSS, was assessed across these repetitions to evaluate the stability and robustness of
278 the model. The range of AUC and TSS values provided insights into how model performance
279 varied with different tuning parameters. The results averaged from these 100 MaxEnt
280 models, were used to create a map identifying favorable areas. This map employs the Habitat
281 Suitability Index (HSI) on a scale from 0 to 1, where low values indicate unsuitable habitat
282 and high values suitable. A contribution percentage from 0 to 100% was assigned to
283 determine the contribution of each environmental variable to the final model. In addition,
284 response curves were generated to visually represent the relationships between
285 environmental variables and the predicted probability of presence for the olive ridley turtle;
286 limiting the model to three class features enabled a relatively straightforward interpretation
287 of these relationships.

288 **2.3.2. SDM projections**

289 The final model results were mapped to the different environmental conditions experienced
290 in the ETP during warm and cold periods. To ensure the model's robustness and validate its
291 overall quality, independent olive ridley turtle records from [Plotkin \(2010\)](#) were used,
292 consisting of 438 presences registered using satellite tags from 21 females and 9 males of
293 olive ridley turtles tagged at Nancite Beach, Costa Rica, between 1990 and 1993. For more
294 details on the used satellite tags and their configuration, see [Plotkin \(2010\)](#) and [Plotkin et al.
295 \(1995\)](#). Although the independent occurrence data did not cover both warm and cold
296 periods, this validation process was crucial for confirming that the model accurately predicts
297 turtle presence beyond the data used for calibration. In this analysis, environmental variables
298 were prepared in the same way as previously but were explained before considering the
299 periods described below. The Extended Reconstructed Sea Surface Temperature v5 (ERSST)
300 dataset was used to identify the specific ENSO scenarios. The ERSST provides a global
301 monthly sea surface temperature (SST) analysis in 2°x2° quadrants derived from the

302 International Comprehensive Ocean-Atmosphere Dataset (ICOADS) ([Huang et al., 2017](#)).
303 Quadrants with available turtle records were selected to obtain more detailed temperature
304 information, and to locate extreme temperature changes in areas known to be selected by
305 the species. This approach helped in identifying shifts in potential habitat distribution in
306 response to environmental changes. The average year was calculated for the period 1990-
307 2021 to obtain monthly anomalies per quadrant (Appendix 2). Then, 3-month moving
308 averages were obtained and plotted for each quadrant and the average for all the selected
309 quadrants. Based on the Oceanic El Niño Index definition (ONI) ([NOAA, 2023](#)), periods with
310 anomalies > 0.5 °C were considered warm, and periods with anomalies < -0.5 °C were
311 considered cold. This approach identified a warm period from January 2019 to January 2020
312 and a neutral period (anomalies between -0.5 and 0.5 °C) from January 2020 to December
313 2021. Extreme scenarios such as El Niño 1997 and La Niña 1999 were also considered
314 (Appendix 3).

315 Projecting MaxEnt results to conditions beyond those used to create the model can use three
316 different strategies: (1) No extrapolation, which considers that all conditions outside the
317 calibration range are unsuitable; (2) Extrapolation with restraint, which extrapolates
318 marginal values within the calibration area as predictions for more extreme conditions; and
319 (3) Unconstrained extrapolation, which extends the response curve based on environmental
320 trends during the study period. To choose the optimal strategy based on the results, we
321 calculated the extrapolation risk in transfers between present and El Niño and La Niña
322 scenarios through the mobility-oriented parity (MOP) using the *kuenm_mop* function.
323 According to [Owens et al. \(2013\)](#), besides extrapolation risk, this function also calculates the
324 environmental differences between the environmental range used to construct the model
325 (calibration region) and the transfer scenarios (ENSO periods). Based on these results, we
326 chose an extrapolation strategy to create binary maps that represent changes in the
327 potential distribution of the species according to three categories: (1) Lost or contracted
328 areas (suitable in the present, but not in the transfer scenario); (2) Gained or expanded areas
329 (not suitable in the present, but suitable in the transfer scenario); and (3) Stable areas
330 (suitable in both the present and transfer scenarios). Subsequently, the results were
331 mapped, and the percentage values of gained, lost, and stable suitable areas for the species
332 were calculated for the transfer scenarios. This analysis allowed for the evaluation of the
333 different extrapolation strategies and their implications for predicting potential distribution
334 shifts of the species under different climate conditions.



335

336 **Fig. 2.** Climatologies of the variables used in the Ecological Niche Model for the olive ridley
 337 turtle *Lepidochelys olivacea* in the Eastern Tropical Pacific Ocean (2009-2011 and 2016-
 338 2018). a) Sea surface temperature; b) chlorophyll-a concentration; c) ocean mixed layer
 339 thickness; d) sea surface height above geoid; and e) current velocity.

340 **3. Results**

341 Oceanographic features in the ETP during the study period, as indicated by the derived
 342 climatologies, indicated that the regions with higher sea surface temperatures were located
 343 to the north of the central Pacific ($> 25\text{ }^{\circ}\text{C}$), while the coldest zones were in the equatorial
 344 region ($< 24\text{ }^{\circ}\text{C}$). Spatial patterns of chlorophyll-a concentration revealed coastal areas as
 345 regions with higher productivity ($> 1\text{ mg} \cdot \text{m}^{-3}$). The mixed layer thickness remained around
 346 10 m deep, except at the north and south of the equatorial zone, where it was greater (> 20
 347 m). Current velocity was generally low, ranging from 0 to $0.5\text{ m} \cdot \text{s}^{-1}$, except in the western

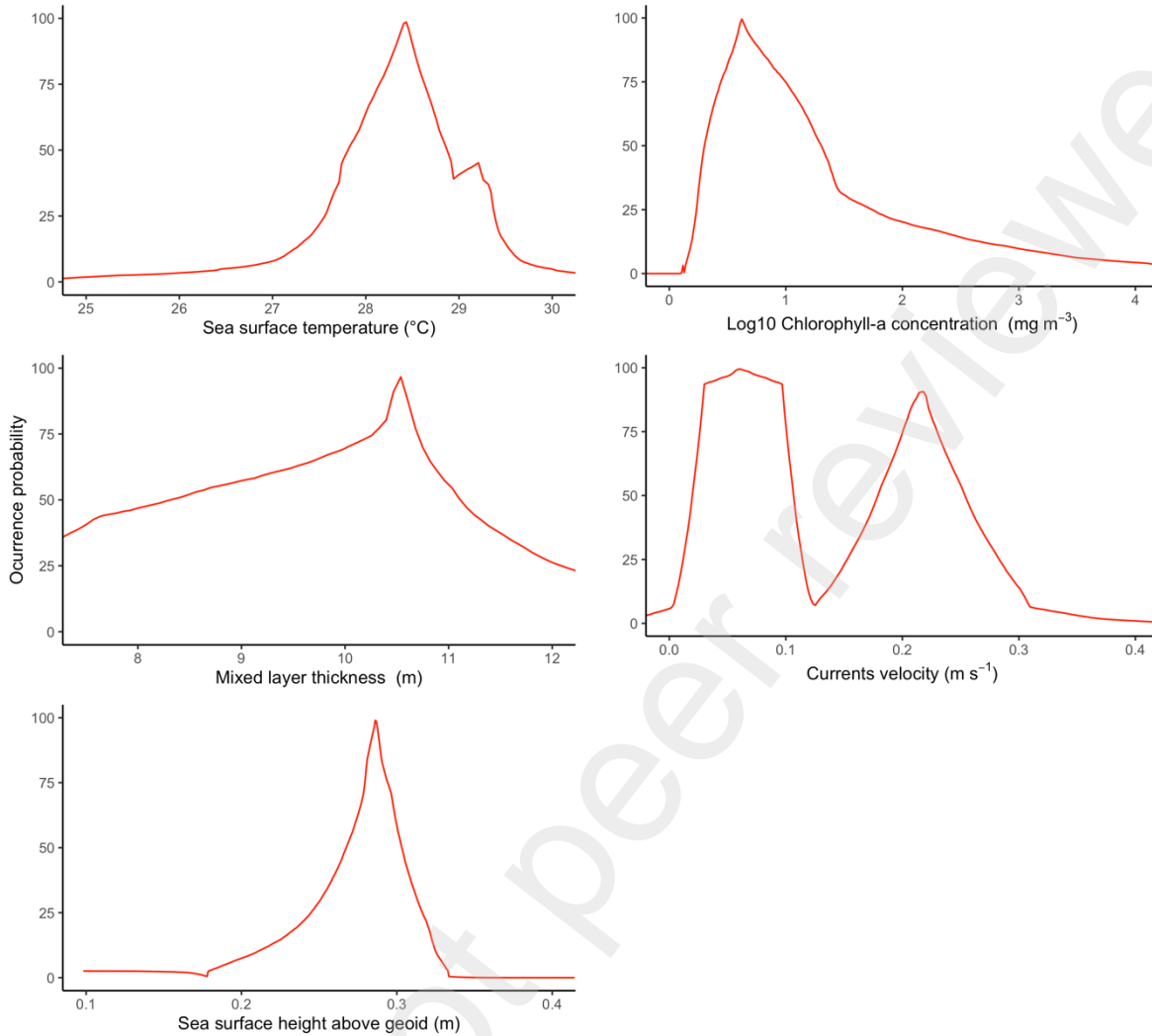
348 Galápagos Islands, where current velocities exceeded $1.0 \text{ m} \cdot \text{s}^{-1}$. Altimetry data showed
349 values close to 0 m throughout the region, particularly in the southern zone (Fig. 2).

350 3.1. Species distribution model

351 A total of 1825 (out of 3492) records of geographic occurrence records were retained to
352 perform the SDM calculations. These records were kept after geographic positions were
353 filtered to remove records according to [Edrén et al. \(2010\)](#) methodology. The best habitat
354 suitability model was obtained with the LQH class and regularization factor 1, showing good
355 predictive potential ($\text{AUC} > 0.87$ for the cross-validated model). The variables with the
356 greatest contribution were \log_{10} -transformed chlorophyll-a concentration (44.7 %) and sea
357 surface temperature (20.2 %) (Table 1). The response curves, which describe the
358 relationships between the probability of presence and the environmental variables, are
359 illustrated in Fig. 3. There is a greater probability of *Lepidochelys olivacea* presence in
360 habitats with a sea surface temperature between 28 -28.5 °C, a chlorophyll-a concentration
361 $< 1 \text{ mg} \cdot \text{m}^{-3}$, a mixed layer thickness between 10 -11 m, sea surface height above geoid
362 around 0.3 m and low currents velocities $< 0.1 \text{ m} \cdot \text{s}^{-1}$.

363 **Table 1** Contribution percentages of the environmental variables used in the final model for
364 the olive ridley turtle *Lepidochelys olivacea* in the Eastern Tropical Pacific and Cross-
365 validation statistics. AUC, Area Under the Curve; AICc, Corrected Akaike Information
366 Criterion.

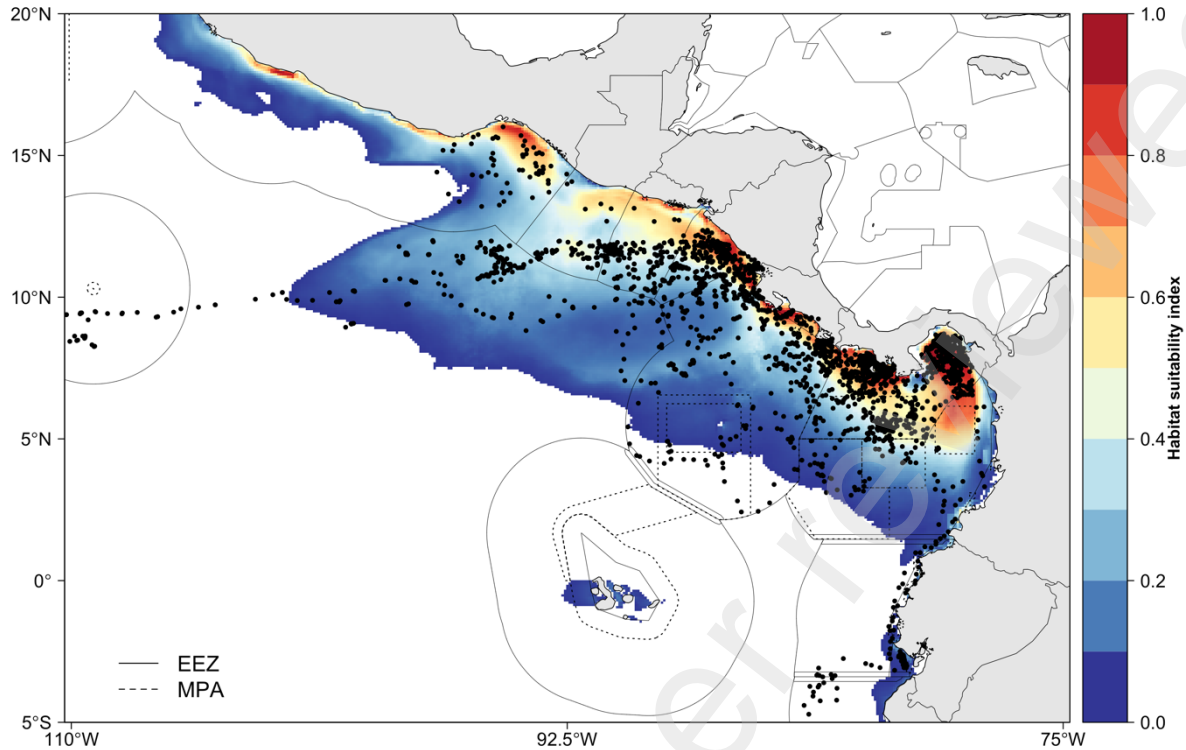
Variable	Contribution average (%)
Chlorophyll-a concentration	44.7
Sea surface temperature	20.2
Mixed layer thickness	18.7
Sea surface height above geoid	13.3
Current velocity	3.2
Validation Statistics	
AUC	0.87
AICc	10.02
Omission rate	0.048
Model	LQH
Regulation factor	1



377

378 **Fig. 3.** Environmental response curves of the environmental variables derived from the
 379 Ecological Niche Model of the olive ridley turtle *Lepidochelys olivacea* in the Eastern Tropical
 380 Pacific. Red curves show how the probability of presence changes as the value of a particular
 381 variable changes; dashed grey lines show higher occurrence probability values.

382 The HSI map highlights suitable areas along the Eastern Pacific coast, including estuarine
 383 systems and close to upwelling-areas (Fig. 4). Based on our post-nesting data, the HSI
 384 suggests that this species is predominantly found near the coast, mainly in proximity to the
 385 nesting sites in Panama and Costa Rica. Also, the Exclusive Economic Zones (EEZ) of Panama,
 386 Costa Rica, Nicaragua, El Salvador, and Guatemala have a high probability of occurrence. In
 387 contrast, the Costa Rica Dome and certain areas close to the Gulf of Tehuantepec show low
 388 HSI values.



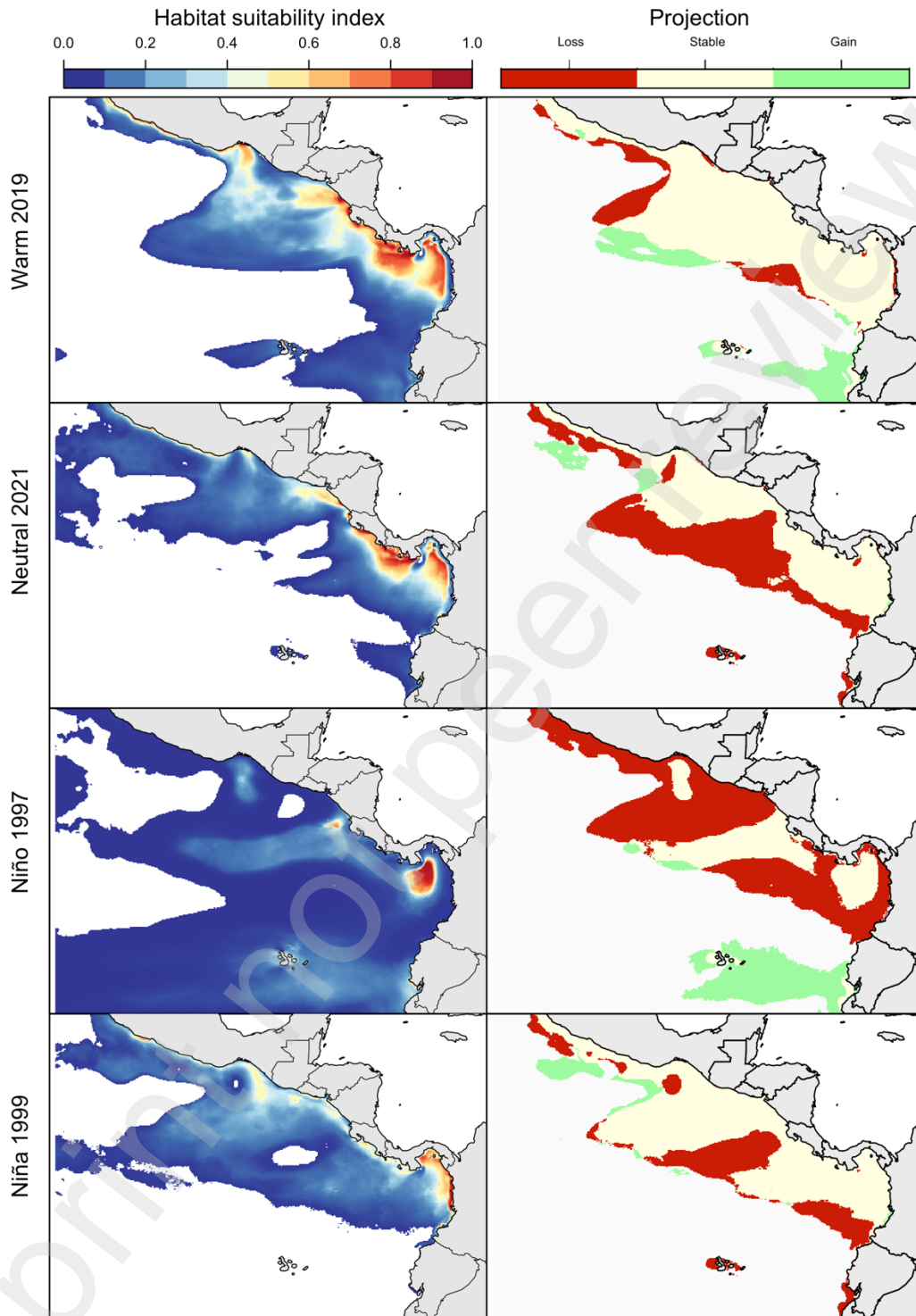
389

390 **Fig. 4.** Habitat suitability index (HSI) of the olive ridley turtle *Lepidochelys olivacea* in the
 391 Eastern Tropical Pacific. Black dots represent satellite telemetry observations (From [Guzman](#)
 392 [et al. \(2019\)](#) and [Figgenger et al. \(2022\)](#)). Grey continuous lines represent the economic
 393 exclusive zones (EEZ), and grey dashed lines the Marine Protected Areas (MPA). The range
 394 of suitability classes are: 0 = not suitable, 0–0.4 = not very suitable, 0.4–0.6 = moderately
 395 suitable, 0.6–0.8 = suitable, and 0.8–1 = highly suitable.

396 3.2. SDM projections

397 Based on the results of the projection, we chose No extrapolation strategy to create binary
 398 maps that represent changes in the potential distribution of the species. These maps indicate
 399 that under neutral conditions (year 2021), the habitat suitability of *Lepidochelys olivacea*
 400 contracted by 12.07% in the central Pacific and coastal areas of Ecuador and Colombia but
 401 increased by 1.16% in oceanic waters to the south of Mexico (Fig. 5). Projections during warm
 402 conditions (2019-2020) experienced a loss of habitat suitability of 3.96% in the central Pacific
 403 and a gain of 5.66% in oceanic zones with a clear expansion towards the south in the
 404 equatorial region. These patterns were accentuated during the ENSO events of El Niño 1997
 405 and La Niña 1999. The El Niño scenario 1997 showed a pattern like the warm period of 2019-
 406 2020 but with a habitat extent loss of 18.57% in the central Pacific and a gain of 7.3% in the
 407 equatorial zone. The La Niña scenario 1999 was like the neutral period of 2021, showing a
 408 loss of habitat suitability by 7.54% in the central Pacific oceanic areas. The gain during this
 409 period reached 1.73% and was localized towards the oceanic waters to the south of Mexico.
 410 These changes were related to variations in sea surface temperature and chlorophyll-a

411 concentration in the region, with high HSI values observed in areas with high chlorophyll-a
412 production during warm and cold periods. However, the relationship was inverse for zones
413 with high thermal variability. For example, during warm periods, areas with high sea surface
414 temperatures showed a loss of suitability, and during cold periods, areas with low
415 temperatures were also considered less favorable for the species.



416

417 **Fig. 5.** Results of the SDM projections of the potential distribution of the olive ridley turtle
 418 *Lepidochelys olivacea* in the Eastern Tropical Pacific, during cold and warm periods (warm
 419 period 2019, neutral period 2021, El Niño event of 1998, and La Niña event of 1999).

420 4. Discussion

421 Considering the constant warming of the ocean ([IPCC, 2021](#)), understanding the fluctuation
422 in the distribution of a species as a response to changes in oceanographic changes is key to
423 developing decision-support tools for the climate-smart management of marine ecosystems
424 ([Boyce et al., 2022](#)). The present study assessed the conditions that favor or limit the suitable
425 habitat of *Lepidochelys olivacea* in the ETP, showing that chlorophyll-a concentration and sea
426 surface temperature variability are this species' most significant factors. Moreover, our
427 results suggest changes in the oceanographic setting can significantly impact the distribution
428 of this species. Particularly during extreme ENSO events, low productivity, and warmer
429 temperatures forced the projected habitat to contract and move towards southern latitudes
430 and further offshore. These results add to the growing body of literature suggesting a shift
431 in marine species range could occur along the coast of the eastern Pacific Ocean and
432 potentially into more oceanic areas due to a changing climate (e.g. [Clarke et al., 2020](#);
433 [Rodriguez-Burgos et al., 2022](#)).

434 The limitations of this study must be considered in the context of data availability and the
435 nature of the research. For example, the use of satellite telemetry data in SDM has increased
436 due to its greater accuracy and its ability to more precisely align with actual environmental
437 conditions over time, compared to open-access databases that provide similar data on
438 species locations ([Edrén et al., 2010](#); [Pikesley et al., 2013](#)). This temporal alignment enhances
439 the precision of matching environmental conditions to the data. However, it has not yet been
440 widely adopted based on the premise that spatially autocorrelated data can bias the resulting
441 models if not properly dealt with ([Cushman, 2010](#); [Miller et al., 2019](#)). It should be noted that
442 spatial autocorrelation can also be an issue for any kind of data, even open-access databases
443 ([Paradinas et al., 2023](#)). Recently, there has been an increasing effort to explore linking
444 tagging data to SDMs due to the larger amounts of data availability. Furthermore, SDMs
445 implicitly assume that geographic data points for species records are independent ([Phillips
446 et al., 2009](#)), which is not necessarily true regarding telemetry studies where data is
447 temporally and spatially autocorrelated ([Gurarie, 2009](#)). Following [Aarts et al. \(2008\)](#), [Edrén
448 et al. \(2010\)](#), and [Pikesley et al. \(2013\)](#) we attempted to overcome limitations within our data
449 by excluding all satellite positions from the first 48 hours after tagging the individuals, using
450 randomly selecting a fixed number of relocations from each tagged individual, and by
451 including one single relocation per day.

452 Another important factor is the bias associated with the portion of the population under
453 assessment ([Godley et al., 2008](#)). Ideally, in distribution modeling, presence records should
454 represent many portions of the species' population life stages, and range, and be collected
455 in different periods ([Varela et al., 2009](#)). The distribution of *Lepidochelys olivacea* in the ETP
456 has been previously described to span as far as 150° W over the equatorial region. This may
457 suggest that our study might not fully capture the species' ecological niche if certain
458 latitudinal and longitudinal ranges are inadequately represented. [Montero et al. \(2016\)](#)
459 assessed 12 years of bycatch by tuna purse seiners and reported this species was found all
460 across the ETP, yet it was more susceptible to being caught in offshore areas along the

461 equator. Conversely, [Peavey \(2010\)](#) obtained contrasting results by modeling suitable
462 habitats through several statistical tools based on observations collected in front of the coast
463 of Central America and different environmental variables (e.g. sea surface temperature,
464 chlorophyll-a concentration, and bathymetry). The only thing Peavey's models conveyed was
465 high suitability near coastal areas over the continental shelf, which resembles the results
466 obtained in our study. The mismatch between these studies can be attributed to a
467 combination of sampling effort, type of observations, the modeling approach, and species-
468 specific dispersal constraints (the distance of records from shore) ([Matthiopoulos, 2022](#)). Our
469 datasets focused on a large sample of adult males, especially females tagged at different
470 years and locations during and after their nesting season, whose movements covered an
471 important section of its observed distribution ([Montero et al., 2016](#)), including the areas used
472 by early life stages used in the study by [Peavey \(2010\)](#).

473 It is important to note that differences are expected between the observed distribution and
474 the suitable habitat modeled for a species when using tracking data as a proxy in SDMs ([Van
475 Moorter et al., 2023](#)). Tracking data reveals the environmental conditions that individuals
476 seek during different behaviors (e.g. nesting, migrating, foraging) and helps to understand
477 the geographical areas they can access based on their movement and dispersal abilities
478 ([Soberon and Peterson, 2005](#)). In contrast, SDMs typically provide an average measure of
479 habitat suitability across these various behavioral states without distinguishing between
480 them, contrary to the recommendations of [Guisan and Thuiller \(2005\)](#). This can lead to less
481 accurate predictions because the specific needs and habitats preferred during different
482 behavioral states are not individually accounted for. For example, [Pikesley et al. \(2013\)](#),
483 reported a high HSI value of post-nesting olive ridleys over the continental shelf of western
484 Africa, regardless of the individuals displaying long offshore migrations and extended
485 distribution. Their results are similar to ours in that individuals were also observed moving
486 further offshore from Central America, yet coastal areas were depicted as having high HSI.
487 This supports our results as an important first step for a comprehensive understanding of the
488 spatial ecology of sea turtles when dispersing from their nesting sites ([Hays and Hawkes,
489 2018](#)), and for modeling the functional habitat of the ETP populations ([Bruneel et al., 2018](#);
490 [Van Moorter et al., 2023](#)). It is nevertheless recommended that the tagging be expanded to
491 early life stages and individuals traversing offshore feeding grounds to better capture
492 potential connectivity routes back to nesting sites and model the functional habitat of this
493 population.

494 Our results show the habitat of *Lepidochelys olivacea* is characterized by low chlorophyll-a
495 concentration ($< 0.1 \text{ mg} \cdot \text{m}^{-3}$) with low thermal variability (28 - 28.5 °C), slow current velocity
496 ($< 0.2 \text{ m} \cdot \text{s}^{-1}$), a shallow mixed layer thickness (9.5 – 10.5 m), and low sea surface height (0.3
497 m). These results are consistent with [Peavey \(2010\)](#), who, using monthly averaged data in a
498 MaxEnt algorithm, reported that *Lepidochelys olivacea* prefers temperatures a few degrees
499 higher (29.5 - 31.5 °C), which remain suitable in our study (Fig. 3). Other studies in the region
500 showcase diverse habitat preferences due to various types of data and methodologies. For
501 example, [Montero et al. \(2016\)](#) used generalized additive models (GAMs) on catch data to
502 model the response of the natural logarithm of the CPUE to the monthly average of

503 environmental parameters, and highlighted a higher bycatch probability at temperatures
504 ranging from 26 to 30 °C, particularly during sets in areas with low chlorophyll-a
505 concentrations ($< 0.36 \text{ mg} \cdot \text{m}^{-3}$). More recently, [Figgner et al. \(2022\)](#) also used GAMs to
506 model the response of presence and pseudo-absence (derived from telemetry data) to the
507 8-day composites of remotely sensed data and other environmental parameters. Their work
508 indicated temperature preferences for this species in the ETP within the range of 25.5 to 28.5
509 °C. Similarly, [Polovina et al. \(2003\)](#) described a comparable temperature range (24 – 27 °C)
510 based on turtle bycatch in the central North Pacific. They utilized descriptive analyses and
511 spatial interpolation on daily and monthly environmental parameters to analyze the
512 movements and habitat preferences of loggerhead and olive ridley turtles. In Costa Rica,
513 [Swimmer et al. \(2009\)](#) used a Kalman filter state-space model to analyze light-based
514 longitude and latitude data, incorporating sea surface temperatures and chlorophyll
515 concentrations. They found that most turtles were associated with sea surface temperatures
516 between 25 and 28 °C, and chlorophyll concentrations below $0.4 \text{ mg} \cdot \text{m}^{-3}$. They used satellite
517 data with a daily and weekly resolution. [Guzman et al. \(2019\)](#) extended this analysis by
518 employing a Hidden Markov Model to differentiate between behavioral states and found
519 significant variations in monthly chlorophyll-a concentrations. Their results indicate that
520 tracked turtles foraged in areas with notably higher chlorophyll-a concentrations ($0.91 \text{ mg} \cdot$
521 m^{-3}) compared to the concentrations during migration ($0.41 \text{ mg} \cdot \text{m}^{-3}$). Despite these
522 variations, the results across studies underscore the importance of diverse data types and
523 methodologies in achieving a comprehensive understanding of the spatial ecology of
524 *Lepidochelys olivacea* and highlighting the species' flexible habitat preferences.

525 In our study, chlorophyll-a concentration is the key variable that defines the presence of this
526 species in the ETP. *Lepidochelys olivacea* is not a specialized herbivore or phytoplanktivore
527 ([Peavey et al., 2017](#)), but productivity hotspots are likely to also aggregate higher trophic
528 levels species, including prey items. Other SDM studies in the North Atlantic and the ETP also
529 highlight oceanic frontal activity and chlorophyll-a concentration as the most significant
530 variables for this species ([Peavey, 2010](#); [Pikesley et al., 2013](#)). The preferences for
531 chlorophyll-a concentrations are similarly reflected in the GAM models by [Figgner et al.](#)
532 [\(2022\)](#), who associated a higher presence of the species with euphotic depths (30 m)
533 alongside elevated levels of particulate organic and inorganic carbon. However, the role of
534 chlorophyll-a concentration in sea turtle distribution has not yet been fully elucidated. Like
535 other predators, *Lepidochelys olivacea* does not feed directly on phytoplankton, but it does
536 opportunistically on jellyfish and demersal prey in deep neritic and shallow pelagic waters
537 ([Echevengúá et al., 2023](#)). Given individuals of this species starve during mating and breeding
538 season ([Santoro and Meneses, 2007](#)), it is likely that post-nesting individuals are in search of
539 highly productive waters to feed on nutrient-rich prey items that will aid them in recovering
540 optimal physiological health ([Espinoza-Romo et al., 2018](#)).

541 It is important to note that seasonal upwelling areas, such as the Gulf of Tehuantepec and
542 the Costa Rica Thermal Dome, were modeled as marginal suitable habitats. The seasonal
543 dynamics of these systems likely impact the species' habitat selection. The Tehuantepecer
544 winds, prevalent from November to February, induce coastal upwelling and the formation of

545 cyclonic and anticyclonic eddies in the Gulf of Tehuantepec ([Trasviña et al., 1995](#)). Under the
546 influence of these winds, a cold-water plume is generated, extending over 400 km offshore
547 and potentially acting as a natural barrier to the species migration in the region ([Velázquez-
548 Muñoz et al., 2011](#)). The predicted distribution of nesting grounds for this species also
549 showed a marginal suitable habitat over the coast of the Gulf of Tehuantepec ([Pike, 2013](#)),
550 despite hosting an important arribada nesting ground ([Montero et al., 2016](#)). While
551 temperature is considered secondary in importance, its seasonal component could be
552 flagged as marginal areas of much greater importance for the habitat of this species. This
553 relationship with habitat selection processes emphasizes the complexity of these
554 interactions and their role in shaping the species' distribution patterns ([Akesson et al., 2021](#)).

555 The complementary effect of temperature on this species cannot thus be ruled out, as shown
556 by the results presented in our study. Some authors suggest that olive ridley turtles appear
557 resilient to environmental changes ([Ariano-Sánchez et al., 2020](#)) and can quickly recover by
558 adapting to new habitats ([Plotkin, 2010](#)). However, the results of this study indicate that the
559 species may show consistent changes in the geographical extent of its pelagic and neritic
560 suitable habitat in response to environmental variation driven by ENSO events, with one
561 example being its presence in southern latitudes. The ENSO phenomenon is a dominant
562 source of interannual climatic variability in the ETP, inducing significant warming (El Niño)
563 and cooling (La Niña) of the regional sea surface temperature ([Wang and Fiedler, 2006](#)).
564 During El Niño, the southeast trade winds weaken, intensifying the equatorial current that
565 transports warm surface water toward the central Pacific coast ([Wang and Picaut, 2004](#)).
566 According to [Zhang et al. \(2019\)](#) and [Fosu et al. \(2020\)](#), the temperature increase, especially
567 in coastal areas, results in a change in the thermocline and increased stratification, leading
568 to reduced nutrient availability and weakened upwelling below 100 m. During La Niña, the
569 trade winds strengthen, pushing warm coastal waters westward, weakening the equatorial
570 current, while the Peru Current and upwelling intensify. As a result, cold, nutrient-rich waters
571 rise to the surface, cooling the central Pacific ([Fiedler and Lavín, 2017](#)). [Peavey et al. \(2017\)](#)
572 pointed out that habitat alteration could compel the species to travel long distances in search
573 of better environmental conditions and food sources. This is supported by [Montero et al.
574 \(2016\)](#), who observed a relationship between higher catches of olive ridley turtles afar from
575 nesting beaches and over the equatorial region during positive ONI years. The species'
576 nomadic behavior could exacerbate the observed shift in suitable habitat as an adaptation
577 to searching for more productive, less warm waters. Previous studies have shown that this
578 regional environmental variability can also change the dynamics of other pelagic species in
579 the region, some of which are prey for the olive ridley turtle. For example, [Reilly \(1990\)](#)
580 suggested that changes in biological productivity in the ETP can act as a mechanism for
581 vertical aggregation and a biological barrier for fishes and squids, which serve as prey for
582 higher pelagic species such as dolphins. When considering this concept within an ecological
583 framework, changes in oceanographic conditions that influence the suitable habitats of
584 *Lepidochelys olivacea* could have a cascading effect on the entire food web, impacting not
585 only the olive ridley turtle but also its predators and prey.

586 Long-term monitoring is required to expand further our understanding of the effects of
587 regional oceanographic variation and climate change on olive ridley turtle populations. Due
588 to the warming trends in the ETP over the past 40 years ([Zevallos-Rosado et al., 2023](#)), the
589 modeled contraction during ENSO events raises important concerns about how this species
590 will react to permanent and severe productivity and temperature changes over the coming
591 century. [Zevallos-Rosado et al. \(2023\)](#) demonstrated significant changes in regional sea
592 surface temperature since 1982, especially along the continental shelf of Central and South
593 America, exactly the areas where high HSI values were obtained. At the same time, our
594 results suggest that the suitable habitat for this species in the ETP is dynamic and changes
595 spatially and temporally, large-scale climatic variability could lead to strong shifts in the
596 future distribution of olive ridley turtles. These shifts may have significant implications for
597 nesting sites. For instance, while the current data from PROTOMAR-UAS indicate that nesting
598 activity is increasing at certain sites in Mexico ([Sosa-Cornejo et al., 2021](#)), there is a possibility
599 of increased pressure on these sites or the possible displacement of nests from other
600 locations. This could affect both the availability and suitability of nesting sites. Despite these
601 challenges, olive ridley turtles exhibit considerable resilience, with some populations
602 showing an upward trend in nesting abundance even amidst ENSO variability ([Ariano-
603 Sánchez et al., 2020](#)). This resilience is crucial as it suggests that olive ridley turtles may adapt
604 to changing conditions, like other species observed in the region. For instance, the jumbo
605 squid, *Dosidiscus gigas* ([Keyl et al., 2008](#)), and various gastropods ([Rivadeneira and
606 Fernández, 2005](#)) have shown permanent range expansions in response to climate change.
607 Similarly, pelagic fish and sharks are expected to experience permanent range shifts ([Clarke
608 et al., 2020](#); [Rodríguez-Burgos et al., 2022](#)).

609 Range shifts pose a challenge for conservation, as protecting a statically defined spatial area
610 does not necessarily ensure the preservation of the entire population, necessitating a range
611 of complementary conservation measures to ensure a protected seascape ([Tittensor et al.,
612 2019](#)). This is why innovative management approaches may be necessary, where dynamic
613 and effective conservation and management measures are constructed based on climatic
614 conditions. Juvenile and adult bycatch in neritic and oceanic fisheries are a significant threat
615 to olive ridley turtles inhabiting the ETP by artisanal and industrial fisheries ([Caceres-Farias
616 et al., 2022](#)). Although it is challenging to determine definitively the overlap between the
617 ideal habitat and fishing fleets, the results demonstrate the core suitable habitat for post-
618 nesting individuals remains within the EEZs in the region during normal and ENSO conditions.
619 Incorporating fishing effort data could further clarify this relationship. While our study
620 provides valuable insights into the current impacts of ENSO events, it is crucial to consider
621 the broader implications of climate change. The observed shifts in habitat suitability may
622 indicate potential future changes in distribution due to long-term climate trends, which the
623 ecosystem. The SDM allows for the identification of priority conservation areas for this
624 species in the ETP. A deeper understanding of fishing efforts and bycatch would facilitate an
625 integrated approach both within and between countries to enhance existing regional
626 management units from a climate-smart approach.

627

628 **Financial Support**

629 This study was partially funded by Re:wild through the project “Identifying priority areas for
630 conservation in the Eastern Pacific Ocean”, by the Galapagos Conservation Trust through the
631 project “Endangered Sharks of Galapagos”, and by Anonymous through the project “Mexican
632 Pacific Swimways”. Elka García-Rada was supported by a M.Sc. grant from Consejo Nacional
633 de Humanidades, Ciencia y Tecnología of Mexico.

634 **Declaration of competing interest**

635 The authors declare that they have no known competing financial interests or personal
636 relationships that could have appeared to influence the work reported in this paper.

637 **Authors contributions**

638 Authors EGR and CPP contributed to research planning, data analysis, and manuscript
639 writing; authors ABA, CRM, GR, DT, and HV contributed to data analysis and manuscript
640 writing; and authors HG, PP, and CF contributed to data collection and manuscript writing.

641 **Acknowledgments**

642 We would like to thank the US National Science Foundation, the US Fish and Wildlife Service,
643 Texas A&M University, Texas Sea Grant Grants-in-Aid of Graduate Research, PADI Grant
644 #21778, the Lerner-Gray Fund for Marine Research; the International Community
645 Foundation, INGEMAR, S.A., Grupo Eleta, Conservation International, and the Smithsonian
646 Tropical Research Institute. Also, we appreciate the Consejo Nacional de Humanidades,
647 Ciencia y Tecnología of Mexico, the Galapagos Conservation Trust, and an Anonymous donor
648 for the complementary support for this project. Finally, we thank Sofía Ortega García and
649 Claudia Hernández Camacho for the valuable comments and feedback to improve this
650 manuscript.

651 **References**

- 652 Aarts, G., MacKenzie, M., McConnell, B., Fedak, M., Matthiopoulos, J., 2008. Estimating space-use
653 and habitat preference from wildlife telemetry data. *Ecography* 31, 140-160.
- 654 Abreu-Grobois, A., Plotkin, P., 2008. *Lepidochelys olivacea*. The IUCN Red List Threatened Species
655 2008. IUCN.
- 656 Akesson, A., Curtsdotter, A., Eklof, A., Ebenman, B., Norberg, J., Barabás, G., 2021. The importance
657 of species interactions in eco-evolutionary community dynamics under climate change. *Nature*
658 *Communications* 12, 4759.
- 659 Ariano-Sánchez, D., Muccio, C., Rosell, F., Reinhardt, S., 2020. Are trends in Olive Ridley sea turtle
660 (*Lepidochelys olivacea*) nesting abundance affected by El Niño Southern Oscillation (ENSO)
661 variability? Sixteen years of monitoring on the Pacific coast of northern Central America. *Global*
662 *Ecology and Conservation* 24.
- 663 Belkin, I.M., 2009. Rapid warming of Large Marine Ecosystems. *Progress in Oceanography* 81, 207-
664 213.

665 Boyce, D.G., Tittensor, D.P., Garilao, C., Henson, S., Kaschner, K., Kesner-Reyes, K., Pigot, A., Reyes,
666 R.B., Reygondeau, G., Schleit, K.E., Shackell, N.L., Sorongon-Yap, P., Worm, B., 2022. A climate
667 risk index for marine life. *Nature Climate Change* 12, 854-862.

668 Bruneel, S., Gobeyn, S., Verhelst, P., Reubens, J., Moens, T., Goethals, P., 2018. Implications of
669 movement for species distribution models - Rethinking environmental data tools. *Sci Total*
670 *Environ* 628-629, 893-905.

671 Caceres-Farias, L., Resendiz, E., Espinoza, J., Fernandez-Sanz, H., Alfaro-Nunez, A., 2022. Threats and
672 Vulnerabilities for the Globally Distributed Olive Ridley (*Lepidochelys olivacea*) Sea Turtle: A
673 Historical and Current Status Evaluation. *Animals (Basel)* 12.

674 Cai, W., 2014. Increasing frequency of extreme El Niño events due to greenhouse warming. *Nat Clim*
675 *Change* 4, 111-116.

676 Carman, V., Alemany, M., Dassis, M., Seco, J., Prosdocimi, L., Ponce, A., Mianzan, H., Acha, E.,
677 Rodríguez, D., Favero, M., Copello, S., 2016. Distribution of megafaunal species in the
678 Southwestern Atlantic: key ecological areas and opportunities for marine conservation *ICES*
679 *Journal of Marine Science* 73, 1579-1588.

680 Chambault, P., Thoisy, B., Heerah, K., Conchon, A., Barrioz, S., Reis, V., Berzins, R., Kelle, L., Picard,
681 B., Roquet, F., Le Maho, Y., Chevallier, D., 2016. The influence of oceanographic features on the
682 foraging behavior of the olive ridley sea turtle *Lepidochelys olivacea* along the Guiana coast. .
683 *Prog Oceanogr* 142, 58-71.

684 Clarke, T.M., Reygondeau, G., Wabnitz, C., Robertson, R., Ixquiac-Cabrera, M., López, M., Ramírez
685 Coghi, A.R., del Río Iglesias, J.L., Wehrtmann, I., Cheung, W.W.L., Fourcade, Y., 2020. Climate
686 change impacts on living marine resources in the Eastern Tropical Pacific. *Diversity and*
687 *Distributions* 27, 65-81.

688 Cobos, M., Peterson, T., Barve, N., Osorio-Olvera, L., 2019. Kuenm: Ecological Niche Models using
689 Maxent.

690 Colella, S., Böhm, E., Cesarini, C., Garnesson, P., Netting, J., Calton, B., 2022. Global Ocean
691 Chlorophyll, in: Service, C.M. (Ed.).

692 Costanza, A., Guidino, C., Mangel, J., Alfaro-Shigueto, J., Verutes, G., Caillat, M., Samanta, A., Hines,
693 E., 2021. Participatory risk assesment of Humpback Whale (*Megaptera novaeangliea*) and
694 Leatherback turtle (*Dermochelys coriacea*) bycatch in Northern Peru. *Frontiers in Marine Science*
695 8.

696 Coyne, M., Godley, B., 2005. Satellite Tracking and Analysis Tool (STAT): an integrated system for
697 archiving, analyzing and mapping animal tracking data. *Mar. Ecol. Prog. Ser* 30, 1-7.

698 Cushman, S.A., 2010. Animal Movement Data: GPS Telemetry, Autocorrelation and the Need for
699 Path-Level Analysis, *Spatial Complexity, Informatics, and Wildlife Conservation*, pp. 131-149.

700 Dávalos, N., 2021. Uso de hábitat y movimientos migratorios de la tortuga laúd (*Dermochelys*
701 *coriacea*) en el Océano PACífico Oriental. Centro Interdisciplinario de Ciencias Marinas, México,
702 p. 65.

703 Drévillon, M., Fernandez, E., Lellouche, J., 2022. Global Ocean Physics Reanalysis, in: Service, C.M.
704 (Ed.).

705 Echevengúá, P.S.d.C., Petitet, R., Castilhos, J.C., Oliveira, F.L.C., Bugoni, L., 2023. Habitat use of
706 nesting female olive ridley turtles (*Lepidochelys olivacea*) inferred by stable isotopes in eggs.
707 *Journal of Experimental Marine Biology and Ecology* 565.

708 Edrén, S.M.C., Wisz, M.S., Teilmann, J., Dietz, R., Söderkvist, J., 2010. Modelling spatial patterns in
709 harbour porpoise satellite telemetry data using maximum entropy. *Ecography* 33, 698-708.

710 Elith, Phillips, S., Hastie, T., Dudík, M., Chee, Y., Yates, C., 2011. A statistical explanation of MaxEnt
711 for ecologists. *Diversity and Distributions* 17, 43-57.

712 Espinoza-Romo, B.A., Sainz-Hernandez, J.C., Ley-Quinonez, C.P., Hart, C.E., Leal-Moreno, R., Aguirre,
713 A.A., Zavala-Norzagaray, A.A., 2018. Blood biochemistry of olive ridley (*Lepidochelys olivacea*)
714 sea turtles foraging in northern Sinaloa, Mexico. PLoS One 13, e0199825.

715 Esteban, N., Mortimer, J.A., Stokes, H.J., Laloë, J.-O., Unsworth, R.K.F., Hays, G.C., 2020. A global
716 review of green turtle diet: sea surface temperature as a potential driver of omnivory levels.
717 Marine Biology 167, 183.

718 Fiedler, P., Lavín, M., 2017. Oceanographic Conditions of the Eastern Tropical Pacific, in: Glynn, P.W.,
719 Manzello, D.P., Enochs, I.C. (Eds.), Coral Reefs of the Eastern Tropical Pacific: Persistence and
720 Loss in a Dynamic Environment. Springer Netherlands, Dordrecht, pp. 59-83.

721 Figgenger, C., Bernardo, J., Plotkin, P., 2022. Delineating and characterizing critical habitat for the
722 Eastern Pacific olive ridley turtle (*Lepidochelys olivacea*): Individual differences in migratory
723 routes present challenges for conservation measures. Frontiers in Ecology and Evolution 10, 721.

724 Fosu, B., He, J., Liguori, G., 2020. Equatorial Pacific Warming Attenuated by SST Warming Patterns
725 in the Tropical Atlantic and Indian Oceans. Geophysical Research Letters 47, e2020GL088231.

726 Fujisaki, I., Hart, K., Bucklin, D., Iverson, A., Rubio, C., Lamont, M., Miron, R., Burchfield, P.M., Peña,
727 J., Shaver, D., 2020. Predicting multi-species foraging hotspots for marine turtles in the Gulf of
728 Mexico. Endangered Species Research 43.

729 Godley, B.J., Blumenthal, J.M., Broderick, A.C., Coyne, M.S., Godfrey, M.H., Hawkes, L.A., Witt, M.J.,
730 2008. Satellite tracking of sea turtles: Where have we been and where do we go next?
731 Endangered Species Research 4, 3-22.

732 Graham, R., 2014. The role of Southern Ocean fronts in the global climate system.

733 Guisan, A., Thuiller, W., 2005. Predicting species distribution: offering more than simple habitat
734 models. Ecology Letters 8, 993-1009.

735 Guo, J., 2014. Modelling loggerhead sea turtle *Caretta caretta* nesting habitat. Evaluation of the
736 species distribution model by species-environment and abundance-occupancy relationships.
737 University of Twente, Netherlands.

738 Gurarie, E., 2009. A novel method for identifying behavioural changes in animal movement data.
739 Ecol. Lett 12, 395-408.

740 Guzman, H.M., Rogers, G., Gomez, C.G., 2019. Behavioral States Related to Environmental
741 Conditions and Fisheries During Olive Ridley Turtle Migration From Pacific Panama. Frontiers in
742 Marine Science 6.

743 Hays, G.C., Hawkes, L.A., 2018. Satellite Tracking Sea Turtles: Opportunities and Challenges to
744 Address Key Questions. Frontiers in Marine Science 5.

745 Huang, Brooke, B., Li, J., 2011. Performance of predictive models in marine benthic environments
746 based on predictions of sponge distribution on the Australian continental shelf. Ecological
747 Informatics 6, 205-216.

748 Huang, Thorne, P., Banzon, V., Boyer, T., Chepurin, G., Lawrimore, M., Menne, M., Smith, T., Vose,
749 R., Zhang, H., 2017. NOAA Extended Reconstructed Sea Surface Temperature (ERSST), Version 5.,
750 in: Information, N.N.C.f.E. (Ed.).

751 IPBES, 2019. Global assessment report on biodiversity and ecosystem services of the
752 Intergovernmental Science-Policy Platform on Biodiversity and Ecosystem Services. IPBES
753 secretariat, Bonn, Germany.

754 IPCC, 2021. Climate Change 2021: The Physical Science Basis. Contribution of Working Group I to
755 the Sixth Assessment Report of the Intergovernmental Panel on Climate Change. Cambridge
756 University Press. In Press.

757 Jiménez-Valverde, A., Peterson, A., Soberón, J., Overton, J., Aragón, P., Lobo, J., 2011. Use of niche
758 models in invasive species risk assessments. Biological Invasions 13, 2785-2797.

759 Keyl, F., Argüelles, J., Mariátegui, L., Tafur, R., Wolff, M., Yamashiro, C., 2008. A Hypothesis on Range
760 Expansion and Spatio-Temporal Shifts in Size-at-Maturity of Jumbo Squid
761 (*Dosidicus gigas*) in the Eastern Pacific Ocean, Reports. California Cooperative Oceanic Fisheries
762 Investigations, La Jolla, CA, USA.

763 Lavín, M., Fiedler, P., Amador, J., Ballance, L., Farber, J., Mestas-Nuñez, A., 2006. A review of eastern
764 tropical Pacific oceanography: Summary. *Progress in Oceanography* 69, 391-398.

765 Leroy, B., Meynard, C., Bellard, C., Courchamp, F., 2015. virtualspecies, an R package to generate
766 virtual species distributions. *Ecography*.

767 Luschi, P., Hays, G.C., Papi, F., 2003. A review of long-distance movements by marine turtles, and
768 the possible role of ocean currents. *Oikos* 103, 293-302.

769 Mancino, C., Canestrelli, D., Maiorano, L., 2022. Going west: Range expansion for loggerhead sea
770 turtles in the Mediterranean Sea under climate change. *Global Ecology and Conservation* 38.

771 Matthiopoulos, J., 2022. Defining, estimating, and understanding the fundamental niches of
772 complex animals in heterogeneous environments. *Ecological Monographs* 92.

773 Maurer, A., Seminoff, J., Stapleton, C., Godfrey, M., Burford, M., 2021. Population viability of sea
774 turtles in the context of global warming. *Bioscience* 20, 1-15.

775 McMahan, C., Bradshaw, C., Hays, G., 2007. Satellite tracking reveals unusual diving characteristics
776 for a marine reptile, the olive ridley turtle *Lepidochelys olivacea*. *Marine Ecology Progress Series*
777 329, 239-252.

778 McPhaden, M., Zebiak, S., Glantz, M., 2009. ENSO as an integrating concept in earth science. *Science*
779 314, 1740-1745.

780 McPhaden, M.J., Santoso, A., Cai, W., 2020. El Niño Southern Oscillation in a Changing Climate.
781 American Geophysical Union, Hoboken, NJ, USA.

782 Miller, D.A.W., Pacifici, K., Sanderlin, J.S., Reich, B.J., Gardner, B., 2019. The recent past and
783 promising future for data integration methods to estimate species' distributions. *Methods in*
784 *Ecology and Evolution* 10, 22-37.

785 Montero, J., Martinez-Rincon, R., Heppell, S., Hall, M., Ewal, M., 2016. Characterizing environmental
786 and spatial variables associated with the incidental catch of olive ridley (*Lepidochelys olivacea*)
787 in the Eastern Tropical Pacific purse-seine fishery. *Fish. Oceanogr* 25, 1-14.

788 Morales, N.S., Fernández, I.C., Baca-González, V., 2017. MaxEnt's parameter configuration and small
789 samples: are we paying attention to recommendations? *PeerJ* 5, e3093.

790 Muscarella, R., Galante, P., Soley-Guardia, M., Boria, R., Kass, J., Uriarte, M., Anderson, A., 2014.
791 ENMeval: An R package for conducting spatially independent evaluations and estimating optimal
792 model complexity for Maxent ecological niche models. *Methods in Ecology and Evolution* 5,
793 1198-1205.

794 NOAA, 2023. Cold and warm episodes by season.

795 Olson, S., Jansen, M.F., Abbot, D.S., Halevy, I., Goldblatt, C., 2022. The Effect of Ocean Salinity on
796 Climate and Its Implications for Earth's Habitability. *Geophysical Research Letters* 49,
797 e2021GL095748.

798 Owens, H., Campbell, L., Dornak, L., Saupe, E., Barve, N., Soberón, J., Ingenloff, K., Lira-Noriega, A.,
799 Hensz, C., Myers, C., Peterson, T., 2013. Constraints on interpretation of ecological niche models
800 by limited environmental ranges on calibration areas. *Ecological Modelling* 263, 10-18.

801 Paradinas, I., Illian, J.B., Alonso-Fernández, A., Pennino, M.G., Smout, S., 2023. Combining fishery
802 data through integrated species distribution models. *ICES Journal of Marine Science* 80, 2579-
803 2590.

804 Patrício, A., Varela, M., Barbosa, C., Broderick, C., Catry, P., Hawkes, L., Regalla, A., Godley, B., 2019.
805 Climate change resilience of a globally important sea turtle nesting population. *Global Change*
806 *Biology* 25, 522-535.

807 Pearson, R., Dawson, T., 2003. Predicting the impacts of climate change on the distribution of
808 species: are bioclimate envelope models useful? *Global Ecology and Biogeography* 12, 361-371.

809 Peavey, L., 2010. Predicting Pelagic Habitat with Presence-only Data using Maximum Entropy for
810 Olive Ridley Sea Turtles in the Eastern Tropical Pacific. Duke University.

811 Peavey, L., Popp, B., Pitman, R., Gaines, S., Arthur, K., Kelez, S., Seminoff, J., 2017. Opportunism on
812 the High Seas: Foraging Ecology of Olive Ridley Turtles in the Eastern Pacific Ocean. *Frontiers in*
813 *Marine Science* 4, 348.

814 Pennington, J., Mahoney, K., Kuwahara, V., Kolber, D., Calienes, R., Chavez, F., 2006. Primary
815 production in the eastern tropical Pacific: A review. *Progress in Oceanography* 69, 285-317.

816 Phillips, S., Anderson, R., Schapire, R., 2006. Maximum entropy modeling of species geographic
817 distribution. *Ecological Modelling* 190, 231-259.

818 Phillips, S.J., Dudík, M., Elith, J., Graham, C.H., Lehmann, A., Leathwick, J., Ferrier, S., 2009. Sample
819 selection bias and presence-only distribution models: implications for background and pseudo-
820 absence data. *Ecological Applications* 19, 181-197.

821 Pike, D.A., 2013. Climate influences the global distribution of sea turtle nesting. *Global Ecology and*
822 *Biogeography* 22, 555-566.

823 Pikesley, S., Maxwell, S., Pendoley, K., Costa, P., Coyne, M., Formia, A., Godley, B., Klein, W.,
824 Makanga-Bahouna, W., Maruca, S., Ngouesso, S., Parnell, R., Pemo-Makaya, P., Witt, M., 2013.
825 On the front line: integrated habitat mapping for olive ridley sea turtles in the southeast Atlantic.
826 *Diversity and Distributions*, 1-13.

827 Plotkin, P., 2010. Nomadic behaviour of the highly migratory olive ridley sea turtle *Lepidochelys*
828 *olivacea* in the eastern tropical Pacific Ocean. *Endangered Species Research* 13, 33-40.

829 Polovina, J., Balazs, G., Howell, E., Parker, D., Seki, M., Dutton, P., 2003. Forage and migration habitat
830 of loggerhead (*Caretta caretta*) and olive ridley (*Lepidochelys olivacea*) sea turtles in the central
831 North Pacific Ocean. *Fisheries Oceanography* 13, 36-51.

832 Quiñones, J., González-Carman, V., Zeballo, J., Purca, S., Mianzan, H., 2010. Effects of El Niño-driven
833 environmental variability on black turtle migration to Peruvian foraging grounds. *Hydrobiologia*
834 645, 69-79.

835 Rees, A., Al-kiyumi, A., Broderick, A., Papathanasopoulou, N., Godley, B., 2012. Conservation related
836 insights into behavior of the olive ridley sea turtle *Lepidochelys olivacea* nesting in Oman. *Marine*
837 *Ecology Progress Series* 450, 195-205.

838 Reilly, S., 1990. Seasonal changes in distribution and habitat differences among dolphins in the
839 eastern tropical Pacific. *Marine Ecology Progress Series* 66, 1-11.

840 Richardson, A., Silulwane, N., Mitchell-Innes, B., Shillington, F., 2003. A dynamic quantitative
841 approach for predicting the shape of phytoplankton profiles in the ocean. *Progress in*
842 *Oceanography* 59.

843 Rivadeneira, M.M., Fernández, M., 2005. Shifts in southern endpoints of distribution in rocky
844 intertidal species along the south-eastern Pacific coast. *Journal of Biogeography* 32, 203-209.

845 Rodríguez-Burgos, A.M., Briceno-Zuluaga, F.J., Avila Jimenez, J.L., Hearn, A., Penaherrera-Palma, C.,
846 Espinoza, E., Ketchum, J., Klimley, P., Steiner, T., Arauz, R., Joan, E., 2022. The impact of climate
847 change on the distribution of *Sphyrna lewini* in the tropical eastern Pacific. *Mar Environ Res* 180,
848 105696.

849 Rodríguez-Zárate, C., Sandoval-Castillo, J., Sebille, E., Keane, R., Rocha-Olivares, A., Urteaga, J.,
850 Beheregaray, L., 2018. Isolation by environment in the highly mobile olive ridley turtle
851 (*Lepidochelys olivacea*) in the eastern Pacific. *Proceedings of the Royal Society B: Biological*
852 *Sciences* 285.

853 Root, T., Price, J., Hall, K., Schneider, S., Rosenzweig, C., Pounds, J., 2003. Fingerprints of global
854 warming on wild animals and plants. *Nature* 421, 57-60.

855 Saba, V., Spotila, J., Chavez, F., Musick, J., 2008. Bottom-up and climatic forcing on the worldwide
856 population of leatherback turtles. *Ecology* 89, 1414-1427.

857 Santidrián, P., Saba, V., Blanco, G., Stock, C., Paladino, F., Spotila, J., 2012. Climate driven egg and
858 hatchling mortality threaten survival of Eastern Pacific leatherback turtles. *Plos One* 7, e37602.

859 Santidrián-Tomillo, L., Fonseca, M., Ward, N., Tankersley, N., Robinson, C., Orrego, F., Paladino, V.,
860 2020. The impacts of extreme El Niño events on sea turtle nesting populations. *Climatic Change*
861 159, 163-176.

862 Santoro, M., Meneses, A., 2007. Haematology and plasma chemistry of breeding olive ridley sea
863 turtles (*Lepidochelys olivacea*). *The Veterinary record* 161, 818–819.

864 Seminoff, J., Alfaro-Shigueto, J., Amarocho, D., Arauz, R., Baquero, A., Chacón, D., Gaos, A., Kelez, S.,
865 Mangel, J., Urteaga, J., Wallace, B., 2012. *Biology and Conservation of sea turtles in the Eastern*
866 *Pacific Ocean*. University of Arizona Press, pp. 11-38.

867 Simantiris, N., 2024. The impact of climate change on sea turtles: Current knowledge,
868 scientometrics, and mitigation strategies. *Science of The Total Environment* 923, 171354.

869 Soberon, J., Peterson, A.T., 2005. Interpretation of Models of Fundamental Ecological Niches and
870 Species' Distributional Areas. *Biodiversity Informatics* 2.

871 Sosa-Cornejo, I., Martín-del-Campo, R., Contreras-Aguilar, H.R., Enciso-Saracho, F., González-
872 Camacho, Z.B., Guardado-González, J.I., Campista-León, S., Peinado-Guevara, L.I., 2021. Nesting
873 trends of olive ridley sea turtles *Lepidochelys olivacea* (Testudinata: Cheloniidae) on two beaches
874 in Northwestern Mexico after 30 and 40 years of conservation. *Revista de Biología Tropical* 69,
875 1124–1137.

876 Swimmer, Y., McNaughton, L., Foley, D., Moxey, L., Nielsen, A., 2009. Movements of olive ridley sea
877 turtles *Lepidochelys olivacea* and associated oceanographic features as determined by improved
878 light-based geolocation. *Endangered Species Research* 10, 245-254.

879 Team, R.C., 2023. R: A language and environment for statistical computing. In. Vienna, Austria: R
880 Foundation for Statistical Computing.

881 Tittensor, D., Beger, M., Boerder, K., Boyce, D., Cavanagh, R., Cosandey-Godin, A., Ortuno Crespo,
882 G., Dunn, D., Giffary, W., Grant, S., Hannah, L., Halpin, P., Harfoot, M., Heaslip, S., Jeffery, N.,
883 Kingston, N., Lotze, H., McGowan, J., McLeod, E., Worm, B., 2019. Integrating climate adaptation
884 and biodiversity conservation in the global ocean. *Science Advances* 5, eaay9969.

885 Trasviña, A., Barton, E., Brown, J., Velez, H., Kosro, P.M., Smith, R.L., 1995. Offshore wind forcing in
886 the Gulf of Tehuantepec, Mexico: The asymmetric circulation. *Journal of Geophysical Research:*
887 *Oceans* 100, 20649-20663.

888 Van Moorter, B., Kivimaki, I., Panzacchi, M., Saura, S., Brandao Niebuhr, B., Strand, O., Saerens, M.,
889 2023. Habitat functionality: Integrating environmental and geographic space in niche modeling
890 for conservation planning. *Ecology* 104, e4105.

891 Varela, S., Rodríguez, J., Lobo, J.M., 2009. Is current climatic equilibrium a guarantee for the
892 transferability of distribution model predictions? A case study of the spotted hyena. *Journal of*
893 *Biogeography* 36, 1645-1655.

894 Velázquez-Muñoz, F., Martínez, J., Chavanne, C., Durazo, R., Flament, P., 2011. Wind-driven coastal
895 circulation in the Gulf of Tehuantepec, Mexico. *Ciencias Marinas* 37, 443-456.

896 Villalobos, H., González-Rodríguez, E., 2020. *satIn: Visualisation and Analysis of Ocean Data Derived*
897 *from Satellites*, p. R package version 1.0.

898 Wang, Picaut, J., 2004. Understanding ENSO Physics - A Review, in: Wang, C., Xie, P., Carton, A. (Eds.),
899 *Earth's Climate: The Ocean-Atmosphere Interaction*. Geophysical Monograph Series, AGU,
900 Washington, D. C., pp. 21-48.

901 Wang, C., Fiedler, P.C., 2006. ENSO variability and the eastern tropical Pacific: A review. *Progress in*
902 *Oceanography* 69, 239-266.

903 Wang, G., Cai, W., Gan, B., Wu, L., Santoso, D., Lin, X., Chen, Z., McPhaden, M., 2017. Continued
904 increase of extreme El Niño frequency long after 1.5°C warming stabilization. *Nat Clim Change* 7,
905 568-572.

906 Whiting, S., Long, J., Coyne, M., 2007. Migration routes and foraging behaviour of olive ridley turtles
907 *Lepidochelys olivacea* in northern Australia. *Endangered Species Research* 3, 1-9.

908 Xue, T., Frenger, I., Prowe, A.E.F., José, Y., Oschlies, A., 2021. Mixed layer depth dominates over
909 upwelling in regulating the seasonality of ecosystem functioning in the Peruvian Upwelling
910 System.

911 Zevallos-Rosado, J., Chinacalle-Martínez, N., Carlos Murillo-Posada, J.C., Veelenturf, C.,
912 Peñaherrera-Palma, C., 2023. A comparative analysis of spatiotemporal trends in sea surface
913 temperature in the major marine protected areas of the Eastern Tropical Pacific. *Revista de*
914 *Biología Marina y Oceanografía* 58, 19-31.

915 Zhang, L., Han, W., Karnauskas, K., Meehl, G., Hu, A., Rosenbloom, N., Shinoda, T., 2019. Indian
916 Ocean Warming Trend Reduces Pacific Warming Response to Anthropogenic Greenhouse Gases:
917 An Interbasin Thermostat Mechanism. *Geophysical Research Letters* 46, 10882-10890.

918